International Journal of Mass Spectrometry 377 (2015) 201–204

Contents lists available at ScienceDirect

International Journal of Mass Spectrometry

journal homepage: www.elsevier.com/locate/ijms

Surface induced dissociation yields substructure of *Methanosarcina thermophila* 20S proteasome complexes

Xin Ma [a], Joseph A. Loo [b], Vicki H. Wysocki [a,*]

[a] Department of Chemistry and Biochemistry, The Ohio State University, Columbus, OH 43210, United States
[b] Department of Biological Chemistry, Department of Chemistry & Biochemistry, and UCLA/DOE Institute for Genomics and Proteomics, University of California, Los Angeles, CA 90095, United States

ARTICLE INFO

Article history:
Received 9 April 2014
Received in revised form 11 September 2014
Accepted 12 September 2014
Available online 20 September 2014

Keywords:
Native mass spectrometry
Surface induced dissociation
20S Proteasome
Stacked ring
Charge reduction
Triethylammonium acetate

ABSTRACT

Native mass spectrometry (MS) and surface induced dissociation (SID) have been applied to study the stoichiometry and quaternary structure of non-covalent protein complexes. In this study, *Methanosarcina thermophila* 20S proteasome, which consists of four stacked heptameric rings ($\alpha_7\beta_7\beta_7\alpha_7$ symmetry), has been selected to explore the SID dissociation pattern of a complicated stacked ring protein complex. SID produces both α and β subunits while collision induced dissociation (CID) produces only highly charged α subunit. In addition, the charge reduced 20S proteasome produces the $\alpha_7\beta_7$ fragment, reflecting the stacked ring topology of the complex. The combination of SID and charge reduction is shown to be a powerful tool for the study of protein complex structure.

© 2014 Published by Elsevier B.V.

1. Introduction

Ring and stacked ring structures are common in protein complexes. Understanding the quaternary structure of protein complexes is necessary for defining their structure–function relationship. Native mass spectrometry (MS) with electrospray ionization (ESI) has been coupled with tandem mass spectrometry (MS/MS) to study the quaternary structure, stoichiometry and conformations of protein complexes [1–7]. Human serum amyloid P (SAP) and GroEL are two examples of stacked ring complexes studied using these techniques. Human serum amyloid P (SAP; 125 kDa) is a pentameric ring structure and the crystal structure is available [8]. Each SAP pentamer has two faces, one contains five α-helices and is referred as the A face; the other one contains five double-calcium binding sites and is referred as the B face [9]. The decamer can be assembled from the A–A interface [8], A–B interface [10], or B–B interface [9]. GroEL is another example of a stacked ring structure, as shown by crystallography results. It is a tetradecameric protein complex (801 kDa) consisting of two heptamer rings [11]. GroEL has served as a large protein complex model system for gas phase studies [12–15] and both ion mobility (IM)-MS and CID have been employed to study GroEL ligand binding properties [16–18].

CID of stacked ring protein complexes generally follows the typical asymmetric dissociation pattern to produce highly charged monomer and their corresponding $(n-1)$ mer fragments for SAP decamer [19] and GroEL tetradecamer [15,18,20]. Therefore, CID provides limited information about its three-dimensional structure. SID was employed as a complementary activation method to dissociate these protein complexes. SID of SAP decamer gives not only monomer, but also dimer, tetramer and hexamer, presumably because the ring–ring interaction between monomers is stronger than the monomer–monomer interface in a single ring [19]. In addition, SID of GroEL tetradecamer produces a wide variety of fragments. The charge reduced (by adding triethylammonium acetate, TEAA [21,22]) GroEL tetradecamer precursor in particular produces significant abundance of heptamer, reflecting the native ring–ring topology [23]. These results show SID's potential to characterize the structure of stacked ring protein complexes.

20S proteasomes, which are large stacked ring structure protein complexes, are studied here to explore the SID dissociation pattern and to determine whether substructure information is provided. The 20S proteasome is the core particle of the proteasome, and is a large energy dependent protease found in all three domains of life [24]. It is part of the ubiquitin–proteasome pathway the cell uses to remove degraded and unwanted

* Corresponding author. Tel.: +1 614 292 8687.
E-mail address: wysocki.11@osu.edu (V.H. Wysocki).

http://dx.doi.org/10.1016/j.ijms.2014.09.011
1387-3806/© 2014 Published by Elsevier B.V.

proteins. The 20S proteasome is composed of structurally related α and β subunits, and the four stacked heptameric rings structure is shared among the three domains of life (archaea, bacteria, and eukaryote domains). The assembly is an $\alpha_7\beta_7\beta_7\alpha_7$ symmetric structure, with the α subunit rings located as the outermost rings and the two β subunit rings sandwiched in between [25,26]. The stacked ring complexes have been observed in X-ray crystal structures for archael, yeast, and mammalian proteasomes [27–29] and electron micrographs of bacterial, archael, yeast, and human proteasomes [30–33]. However, the subunit compositions are different in the three life domains. Eukaryotic 20S proteasome contains seven different α subunits ($\alpha_1 - \alpha_7$) and seven different β subunits ($\beta_1 - \beta_7$) [25,26,30,33–35]. In contrast, the 20S proteasomes in actinobacteria and archaea only have one to two different α subunits and one to two different β subunits [24–27,32,36]. CID has been applied to dissociate the 20S proteasomes from the archaeon *Methanosarcina thermophila*. Typical asymmetric dissociation pathways are observed [37]. Because of the simple composition of the α and β subunits, the *M. thermophila* 20S proteasome is selected for our research. SID is applied to dissociate the 20S proteasome of *M. thermophila* in order to reveal the dissociation pattern of the large stacked ring protein complexes by SID. Unfortunately there is no crystal structure for 20S proteasome from *M. thermophila* but a stacked ring structure would be consistent with the X-ray crystal structures of Archaeon *Thermoplasma acidophilum* [27] and Eukaryote yeast [28]. SID is used here to confirm whether the structure of the 20S proteasome from *M. thermophila* is consistent with these other known crystal structures.

2. Materials and methods

The *M. thermophila* 20S proteasome was purchased from Calbiochem (San Diego, CA). The protein solutions were dialyzed against 1 L of 500 mM ammonium acetate (Sigma–Aldrich, St. Louis, MO) at pH 7 using Slide-A-Lyzer MINI Devices, with a 3.5 kDa molecular weight cut off membrane (Thermo Fisher Scientific Inc., Rockford, IL) at 4 °C overnight. The final concentrations obtained are about 4 μM for the *M. thermophila* 20S proteasome. TEAA was purchased from Sigma–Aldrich (St. Louis, MO) at pH 7 and added into the protein solutions to achieve 0.1/0.9 TEAA/ammonium acetate (v/v, 10 mM/90 mM) for charge reduction experiments [21,22] as indicated in the text.

The experiments were performed on a Synapt G2 HDMS instrument (Waters MS Technologies, Manchester, UK) [38,39] modified to include a custom SID device located before the IM cell as described previously [40]. The ESI capillary voltage was 1.3–1.5 kV, the ion source temperature was ~30 °C, and the source pressure was about 6 mbar. The cone voltage was found to be optimal at 100 V because no significant fragmentation was observed under this cone voltage and relatively strong and distinguishable precursor peaks can be observed. Although these conditions provide stronger signal and better resolved precursor peaks, use of this cone voltage may contribute to some pre-unfolding of the complex in the ion source region and more highly charged monomer in SID spectra.

The trap collision cell flow rate of argon was set at 10 mL/min when collecting mass spectra and CID MS/MS spectra for better transmission efficiency of the high *m*/*z* precursors. The pressure reading of argon in the trap ion guide was $\sim 6.0 \times 10^{-2}$ mbar. The trap flow rate of argon was set to 4 mL/min when collecting SID MS/MS spectra because higher pressure may lead to significant scattering in the SID device and decrease the signal dramatically. The pressure reading of argon in the trap ion guide during SID was $\sim 3.3 \times 10^{-2}$ mbar. CID MS/MS was performed by changing the "Trap CE" in the tune page to accelerate the ions to collide with collision gas and SID MS/MS was performed by tuning the voltages on the electrodes of the SID device to steer the ion beam to collide with the surface and increase the "Trap DC bias", which increases all of the DC offsets on the Trap cell and upstream of the Trap cell, to accelerate the ions into the surface. The flow rate to the helium cell was 120 mL/min. The pressure of nitrogen in the IM cell was 2.2 mbar. The IM wave height and velocity were 16.0 V and 200 ms^{-1}, respectively. The time-of-flight (TOF) analyzer pressure was 7.0×10^{-7} mbar.

3. Results and discussion

The *M. thermophila* 20S proteasome contains identical 27.4 kDa α subunits and identical 21.8 kDa β subunits [32,36,37]. The whole 20S proteasome is thus about 690 kDa. A prevoius CID study has shown that one and two α subunits can dissociate from the complex and form the (20S proteasome-α) and (20S proteasome-2α) fragments [37]. The intact 690 kDa 20S proteasome complex can be preserved under the experimental conditions (Fig. 1). In order to explore the fragmentation patterns of the complex, both CID and SID are performed to dissociate the *M. thermophila* 20S proteasome before and after charge reduction with the addition of 10% TEAA (ammonium acetetate 90 mM, TEAA 10 mM) in solution (Fig. 1). TEAA reduces the number of charges by about 25% (from +53 to +39).

The +53 and charge reduced +39 of the 20S proteasome precursor were selected for CID and SID experiments for comparison of dissociation of different charge states. The CID spectrum at 200 V acceleration voltage and the SID spectrum at 160 V acceleration voltage (Fig. 2) of the +53 precursor are selected to exemplify the CID and SID spectra because of good spectral quality and the fact that remaining precursors can be observed under these conditions. CID of the +53 20S proteasome follows the asymmetric dissociation pattern (Fig. 2a) and produces the 27.4 kDa α subunit and the complementary (20S proteasome-α) fragment, in agreement with previous CID results [37]. Different from CID, a series of charge stripping peaks are observed in SID (Fig. 2b). In addition, SID produces products corresponding to both the 27.4 kDa α subunit and 21.8 kDa β subunit and these products also appear at lower charge states than detected for CID. Low

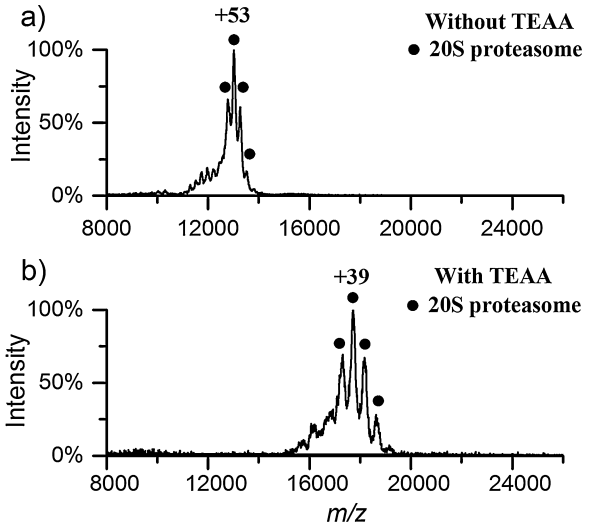

Fig. 1. The mass spectra of *M. thermophila* 20S proteasome before and after charge reduction with 10% (v/v) TEAA in solution.

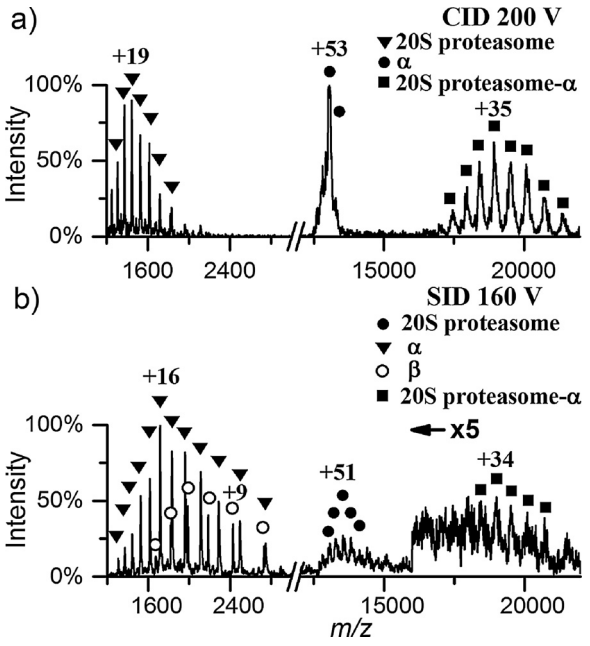

Fig. 2. The MS/MS spectra of +53 charged *M. thermophila* 20S proteasome. The symbols label different charge states of the species indicated in the figure (see legends). (a) CID spectrum at 200 V acceleration voltage (10,600 eV). The α subunit (27.4 kDa) dissociates from the 20S proteasome and complementary (20S proteasome-α) fragment is observed. (b) SID spectrum at 160 V acceleration voltage (8480 eV) with the upper *m/z* region magnified by 5 times. A series of charge stripping peaks of the precursor are observed (the 20S proteasome peaks at lower charge states than the +53 at *m/z* values of approximately 13,000–14,000). Both the α subunit (27.4 kDa) and β subunit (21.8 kDa) are observed in the low *m/z* region of the spectrum. Low abundance (20S proteasome-α) fragment is also observed in the SID spectrum at high *m/z* (17,500–22,000). The S/N is 2–3 in this high *m/z* range, likely, in part, due to the existance of fragments corresponding to loss of β subunits. Possible explanations for the low abundance and poor S/N of high *m/z* (20S proteasome-α) fragments in SID is kinetic energy discrimination in the SID device and the fact that SID produces two product types (loss of α and β) and many more charge states than CID, leading to overlap of peaks and a decrease in abundance for any given peak.

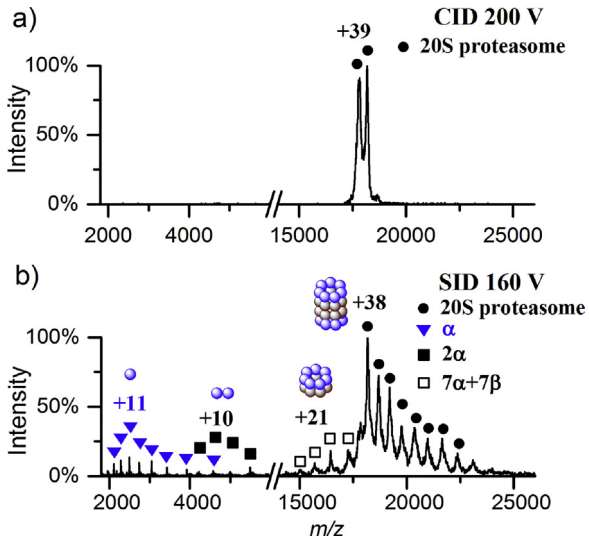

Fig. 3. The MS/MS spectra of +39 charged *M. thermophila* 20S proteasome. (a) CID at 200 V acceleration voltage (7800 eV), which is the highest accessible in the instrument, did not dissociate the +39 20S proteasome. Only one charge stripping peak is observed. (b) SID spectrum at 160 V acceleration voltage (6240 eV). A series of charge stripping peaks of the precursor are observed along with the α subunit (27.4 kDa) as the major monomer fragment observed. A 7α+7β (345 kDa) fragment is observed, consistent with the $\alpha_7\beta_7\beta_7\alpha_7$ structure of the complex.

abundance (20S proteasome-α) fragment is also formed but the (20S proteasome-β) fragment has not been directly observed at the signal-to-noise (S/N) level in the high *m/z* end of the spectrum. Ion mobility failed to further separate different fragments in that *m/z* range (data not shown). Therefore, the (20S proteasome-β) fragment may exist but the amount is lower than the (20S proteasome-α) fragment and is not directly observed. The peak intensities of the α subunit are much stronger than those of the β subunit, supporting the hypothesis that the intensities of the the (20S proteasome-β) peaks are weaker than those of the 20S proteasome-α) fragment. SID allows not only the dissociation of monomer from the outermost α ring, but also from the inner β ring. SID thus provides more structural information about this stacked ring protein complex. However, the wider variety of monomer fragments still does not reflect the existence of the heptameric ring structure in the 20S proteasome. Because a previous SID study of GroEL tetradecamer shows that the combination of charge reduction and SID gives a more dominant separate ring fragment (GroEL heptamer ring) [23], it is desirable to check the SID dissociation pattern of charge reduced *M. thermophila* 20S proteasome.

The CID spectrum at 200 V acceleration voltage and SID spectrum at 160 V acceleration voltage (Fig. 3) of the +39 precursor shows good spectral quality with remaining precursors measurable under these conditions. The 20S proteasome at this charge state does not dissociate at 200 V CID, which is the highest accessible CID acceleration voltage of the instrument. Only one charge stripping peak is observed. In contrast, SID dissociates the 20S proteasome to produce the 27.4 kDa α subunit and, significantly, 345 kDa fragments corresponding to the 7α + 7β subcomplex. A series of charge stripping peaks of the precursor is also observed. Of particular importance is the fact that SID of the charge reduced *M. thermophila* 20S proteasome can break the $\alpha_7\beta_7\beta_7\alpha_7$ 28-mer from the center plane to produce the $\alpha_7\beta_7$ substructure. This information reflects the stacked ring structure and is in agreement with the observation of 7-mer rings for SID of GroEL tetradecamer. It is noteworthy that no individual 7α or 7β ring structures are observed in the SID spectra of *M. thermophila* 20S proteasome presumably because the interaction between the 7α and 7β rings is stronger than that between the two 7β rings. This is consistent with how the 20S proteasome is believed to assemble, with the formation of a 7-member α-ring followed by addition of β subunits to form half proteasomes, which then dimerize to form the intact 20S complex [41]. Of course, this does not preclude the chance that the stability of the gas phase complex is different from its solution phase origins.

4. Conclusion

The combination of SID and charge reduction is shown to be a useful tool to explore the stacked ring structure of 20S proteasome protein complexes. The results agree with the previous SID study of GroEL [23]. SID produces not only the α but also the β subunit from the highly charged (+53) *M. thermophila* 20S proteasome before charge reduction. The most striking result of this work is that SID breaks the charge reduced +39*M. thermophila* 20S proteasome from the center plane to produce $\alpha_7\beta_7$, reflecting the native topology of the complex. Dominant monomers of high charge are also detected, suggesting unfolding (supported by ion mobility results, Fig. S1) as a result of harsh cone voltage conditions and/or SID voltage. Overall, the native MS SID study provides the following information that can allow one to propose the native topology of the complex: (1) The intact *m/z* values correspond to 14α and 14β monomers. (2) An $\alpha_7\beta_7$ fragment is produced. (3) α monomers are

more abundant than β monomers, suggesting that α is more likely on the surface than β. (4) Subspecies such as tetramer plus trimer are not formed, making a ring structure likely (dominant monomers for SID occur from symmetrical ring structures; substructures should occur if they exist, based on other SID data). Taken alone, the information already allows useful speculation on the topology (outer α rings sandwiching interior β rings). When combined with X-ray crystal structures or electron micrographs of related species, the topology is confirmed by the SID results.

More stacked ring protein complexes with well-defined structures should be studied utilizing SID and charge reduction to check whether those ring structures can also be preserved. Based on published SID results for GroEL 14-mer and SAP decamer, plus the *M. thermophila* 20S proteasome results shown here, SID is a useful activation method that splits intact rings from multi-ring protein complexes.

Acknowledgements

This work was financially supported by the National Science Foundation (Grant 0923551 to VHW) and the National Institutes of Health (R01GM103479 to JAL).

Appendix A. Supplementary data

Supplementary data associated with this article can be found, in the online version, at http://dx.doi.org/10.1016/j.ijms.2014.09.011.

References

[1] Z. Hall, C.V. Robinson, Do charge state signatures guarantee protein conformations? J. Am. Soc. Mass Spectrom. 23 (2012) 1161–1168.
[2] A.J. Heck, Native mass spectrometry: a bridge between interactomics and structural biology, Nat. Methods 5 (2008) 927–933.
[3] J.L.P. Benesch, B.T. Ruotolo, F. Sobott, J. Wildgoose, A. Gilbert, R. Bateman, C.V. Robinson, Quadrupole–time-of-flight mass spectrometer modified for higher-energy dissociation reduces protein assemblies to peptide fragments, Anal. Chem. 81 (2008) 1270–1274.
[4] C.S. Kaddis, J.A. Loo, Native protein MS and ion mobility large flying proteins with ESI, Anal. Chem. 79 (2007) 1778–1784.|-|%1e[Accept]
[5] H. Hernandez, C.V. Robinson, Determining the stoichiometry and interactions of macromolecular assemblies from mass spectrometry, Nat. Protoc. 2 (2007) 715–726.
[6] C.N. Pace, S. Trevino, E. Prabhakaran, J.M. Scholtz, Protein structure, stability and solubility in water and other solvents, Philos. Trans. R. Soc. Lond. B Biol. Sci. 359 (2004) 1225–1235.
[7] J.A. Loo, Studying noncovalent protein complexes by electrospray ionization mass spectrometry, Mass Spectrom. Rev. 16 (1997) 1–23.
[8] J. Emsley, H.E. White, B.P. O'Hara, G. Oliva, N. Srinivasan, I.J. Tickle, T.L. Blundell, M.B. Pepys, S.P. Wood, Structure of pentameric human serum amyloid P component, Nature 367 (1994) 338–345.
[9] E. Hohenester, W.L. Hutchinson, M.B. Pepys, S.P. Wood, Crystal structure of a decameric complex of human serum amyloid P component with bound dAMP, J. Mol. Biol. 269 (1997) 570–578.
[10] D. Thompson, M.B. Pepys, I. Tickle, S. Wood, The structures of crystalline complexes of human serum amyloid P component with its carbohydrate ligand, the cyclic pyruvate acetal of galactose, J. Mol. Biol. 320 (2002) 1081–1086.
[11] K. Braig, Z. Otwinowski, R. Hegde, D.C. Boisvert, A. Joachimiak, A.L. Horwich, P.B. Sigler, The crystal structure of the bacterial chaperonin GroEL at 2.8 Å, Nature 371 (1994) 578–586.
[12] J. Fernández de la Mora, Why do GroEL ions exhibit two gas phase conformers? J. Am. Soc. Mass Spectrom. 23 (2012) 2115–2121.
[13] J. Freeke, M.F. Bush, C.V. Robinson, B.T. Ruotolo, Gas-phase protein assemblies: unfolding landscapes and preserving native-like structures using noncovalent adducts, Chem. Phys. Lett. 524 (2012) 1–9.
[14] C.J. Hogan, B.T. Ruotolo, C.V. Robinson, J. Fernandez de la Mora, Tandem differential mobility analysis-mass spectrometry reveals partial gas-phase collapse of the GroEL complex, J. Phys. Chem. B 115 (2011) 3614–3621.
[15] F. Sobott, C.V. Robinson, Characterising electrosprayed biomolecules using tandem-MS—the noncovalent GroEL chaperonin assembly, Int. J. Mass Spectrom. 236 (2004) 25–32.
[16] A. Dyachenko, R. Gruber, L. Shimon, A. Horovitz, M. Sharon, Allosteric mechanisms can be distinguished using structural mass spectrometry, Proc. Natl. Acad. Sci. U. S. A. 110 (2013) 7235–7239.
[17] E. Van Duijn, A. Barendregt, S. Synowsky, C. Versluis, A.J.R. Heck, Chaperonin complexes monitored by ion mobility mass spectrometry, J. Am. Chem. Soc. 131 (2009) 1452–1459.
[18] E. van Duijn, D.A. Simmons, R.H.H. van den Heuvel, P.J. Bakkes, H. van Heerikhuizen, R.M.A. Heeren, C.V. Robinson, S.M. van der Vies, A.J.R. Heck, Tandem mass spectrometry of intact GroEL-substrate complexes reveals substrate-specific conformational changes in the trans ring, J. Am. Chem. Soc. 128 (2006) 4694–4702.
[19] M. Zhou, C. Huang, V.H. Wysocki, Surface-induced dissociation of ion mobility-separated noncovalent complexes in a quadrupole/time-of-flight mass spectrometer, Anal. Chem. 84 (2012) 6016–6023.
[20] T.W. Knapman, V.L. Morton, N.J. Stonehouse, P.G. Stockley, A.E. Ashcroft, Determining the topology of virus assembly intermediates using ion mobility spectrometry-mass spectrometry, Rapid Commun. Mass Spectrom. 24 (2010) 3033–3042.
[21] K. Pagel, S.J. Hyung, B.T. Ruotolo, C.V. Robinson, Alternate dissociation pathways identified in charge-reduced protein complex ions, Anal. Chem. 82 (2010) 5363–5372.
[22] S.J. Allen, A.M. Schwartz, M.F. Bush, Effects of polarity on the structures and charge states of native-like proteins and protein complexes in the gas phase, Anal. Chem. 85 (2013) 12055–12061.
[23] M. Zhou, C.M. Jones, V.H. Wysocki, Dissecting the large noncovalent protein complex GroEL with surface-induced dissociation and ion mobility-mass spectrometry, Anal. Chem. 85 (2013) 8262–8267.
[24] C. Volker, A.N. Lupas, Molecular evolution of proteasomes, in: P. Zwickl, W. Baumeister (Eds.), The Proteasome—Ubiquitin Protein Degradation Pathway, Springer, Berlin, Heidelberg, 2002, pp. 1–22.
[25] J. Maupin-Furlow, Proteasomes and protein conjugation across domains of life, Nat. Rev. Microbiol. 10 (2012) 100–111.
[26] W. Baumeister, J. Walz, F. Zühl, E. Seemüller, The proteasome: paradigm of a self-compartmentalizing protease, Cell 92 (1998) 367–380.
[27] J. Lowe, D. Stock, B. Jap, P. Zwickl, W. Baumeister, R. Huber, Crystal structure of the 20 S proteasome from the archaeon *T. acidophilum* at 3.4 Å resolution, Science 268 (1995) 533–539.
[28] M. Groll, L. Ditzel, J. Lowe, D. Stock, M. Bochtler, H.D. Bartunik, R. Huber, Structure of 20S proteasome from yeast at 2.4 Å resolution, Nature 386 (1997) 463–471.
[29] M. Unno, T. Mizushima, Y. Morimoto, Y. Tomisugi, K. Tanaka, N. Yasuoka, T. Tsukihara, The structure of the mammalian 20S proteasome at 2. 75 resolution, Structure 10 (2002) 609–618.
[30] B. Dahlmann, F. Kopp, P. Kristensen, K.B. Hendil, Identical subunit topographies of human and yeast 20S proteasomes, Arch. Biochem. Biophys. 363 (1999) 296–300.
[31] I. Nagy, T. Tamura, J. Vanderleyden, W. Baumeister, R. De Mot, The 20S proteasome of Streptomyces coelicolor, J. Bacteriol. 180 (1998) 5448–5453.
[32] J.A. Maupin-Furlow, H.C. Aldrich, J.G. Ferry, Biochemical characterization of the 20S proteasome from the Methanoarchaeon *Methanosarcina thermophila*, J. Bacteriol. 180 (1998) 1480–1487.
[33] F. Kopp, K.B. Hendil, B. Dahlmann, P. Kristensen, A. Sobek, W. Uerkvitz, Subunit arrangement in the human 20S proteasome, Proc. Natl. Acad. Sci. U. S. A. 94 (1997) 2939–2944.
[34] L. Huang, A.L. Burlingame, Comprehensive mass spectrometric analysis of the 20S proteasome complex, in: A.L. Burlingame (Ed.), Methods in Enzymology, Academic Press, 2005, 2014, pp. 187–236.
[35] B. Dahlmann, T. Ruppert, P.M. Kloetzel, L. Kuehn, Subtypes of 20S proteasomes from skeletal muscle, Biochimie 83 (2001) 295–299.
[36] J.A. Maupin-Furlow, J.G. Ferry, A proteasome from the *Methanogenic Archaeon Methanosarcina thermophila*, J. Biol. Chem. 270 (1995) 28617–28622.
[37] J. Loo, B. Berhane, C. Kaddis, K. Wooding, Y. Xie, S. Kaufman, I. Chernushevich, Electrospray ionization mass spectrometry and ion mobility analysis of the 20S proteasome complex, J. Am. Soc. Mass Spectrom. 16 (2005) 998–1008.
[38] K. Giles, J.P. Williams, I. Campuzano, Enhancements in travelling wave ion mobility resolution, Rapid Commun. Mass Spectrom. 25 (2011) 1559–1566.
[39] K. Giles, S.D. Pringle, K.R. Worthington, D. Little, J.L. Wildgoose, R.H. Bateman, Applications of a travelling wave-based radio-frequency-only stacked ring ion guide, Rapid Commun. Mass Spectrom. 18 (2004) 2401–2414.
[40] M. Zhou, S. Dagan, V.H. Wysocki, Protein subunits released by surface collisions of noncovalent complexes: nativelike compact structures revealed by ion mobility mass spectrometry, Angew. Chem. Int. Ed. 51 (2012) 4336–4339.
[41] S. Murata, H. Yashiroda, K. Tanaka, Molecular mechanisms of proteasome assembly, Nat. Rev. Mol. Cell Biol. 10 (2009) 104–115.